JOURNAL OF GEOPHYSICAL RESEARCH, VOL. 110, A11312, doi:10.1029/2005JA011064, 2005

D region ionization by lightning-induced electromagnetic pulses

S. B. Mende,[1] H. U. Frey,[1] R. R. Hsu,[2] H. T. Su,[2] A. B. Chen,[2] L. C. Lee,[2] D. D. Sentman,[3] Y. Takahashi,[4] and H. Fukunishi[4]

Received 10 February 2005; revised 31 August 2005; accepted 12 September 2005; published 30 November 2005.

[1] The electromagnetic pulses (EMP) from tropospheric lightning produce transient luminous events (TLEs), known as elves, in the 80–90 km region above the lightning. The luminosity is evidence that the EMP carries sufficient electric field to excite optical emissions at these altitudes; however, it is still unknown whether the field is sufficient to ionize the atmosphere. The first multiwavelength, quantitative observatory on a free-flying satellite dedicated to observing TLEs, the Imager of Sprites and Upper Atmospheric Lightning (ISUAL) instrument on FORMOSAT-2, formerly called ROCSAT-2, confirmed that a significant number of lightning events are accompanied by elves. The instrument consists of a low light level imager and a set of multichannel photometers. In a few cases where the lightning occurred beyond the solid Earth limb, pure spectral measurements of the elves were obtained. Here we analyze such an event and show that the elves contained significant 391.4 nm emission of the N_2^+ ion. This is clear evidence that ionization takes place in elves. The ratio of cross sections for N_2 ionization and the production of the upper state of 391.4 nm emission is not a constant for low-energy electrons found in TLEs. We attempted to find this ratio by comparing our photometric measurements of the TLE produced emissions to theoretically derived emission intensities. The electron energy distribution and the ratios of the modeled N_2 Lyman-Birge-Hopfield (LBH) and the N_2^+ first negative to the second positive were computed as a function of the reduced electric field. From these ratios it was possible to obtain the reduced electric field from the ratios. We estimated that the reduced electric field, which characterizes the local electron energy distribution, was >200 Td. We also made comparisons of the theoretically derived intensities to our measurements of the N_2^+ first positive and Lyman-Birge-Hopfield (LBH) band emission in the elves. On the basis of the ratio between the N_2^+ first negative emission and the time-integrated ionization production, we estimate that the elves produced an average electron density of 210 electrons cm^{-3} over a large (165 km diameter) circular region having an assumed 10 km altitude extent. These observations indicate that thunderstorms are a significant source of ionization in the low- to midlatitude nighttime *D* region.

Citation: Mende, S. B., H. U. Frey, R. R. Hsu, H. T. Su, A. B. Chen, L. C. Lee, D. D. Sentman, Y. Takahashi, and H. Fukunishi (2005), *D* region ionization by lightning-induced electromagnetic pulses, *J. Geophys. Res.*, *110*, A11312, doi:10.1029/2005JA011064.

1. Introduction

[2] The first so-called "elves," a type of transient luminous event (TLE), were seen on the space shuttle [*Boeck et al.*, 1992]. Elves were also seen later by ground-based observers who named them "elves," which is an acronym for Emission of Light and VLF perturbations due to EMP Sources [*Fukunishi et al.*, 1996]. When intense cloud to ground (CG) lightning occurs, an electromagnetic pulse (EMP) is produced. The electric field in the EMP wave accelerates ambient electrons leading to optical emissions in higher-altitude regions above the lightning where the field of the EMP exceeds that of the local critical field to create excitation and ionization [*Inan et al.*, 1991; *Taranenko et al.*, 1993a, 1993b; *Rowland et al.*, 1995; *Inan et al.*, 1996]. If the lightning discharge is equivalent to a vertical current pulse, then the resulting EMP will be emitted preferentially in the horizontal direction. *Inan et al.* [1996] modeled the intensity and distribution of luminosity created by such EMP and predicted that a short burst of emission >10 MR would be seen in the red N_2 first positive band accompanied by considerable ionization [*Barrington-Leigh and Inan*, 1999].

[1]Space Science Laboratory, University of California, Berkeley, Berkeley, California, USA.
[2]Department of Physics, National Cheng Kung University, Tainan, Taiwan.
[3]Geophysical Institute, University of Alaska Fairbanks, Fairbanks, Alaska, USA.
[4]Department of Geophysics, Tohoku University, Sendai, Japan.

0148-0227/05/2005JA011064$09.00

Table 1. ISUAL Filters[a]

Channel Number	Nominal Filter	10% Lower Limit, nm	10% Upper Limit, nm	Purpose
		Imager Filter Used in the Measurement		
1	N_2 1PG	622.8	754	N_2 first positive band filter with some N_2^+ Meinel contribution
		Spectrophotometer (SP) Channels		
1	FUV	150	280	Exploratory observations at high altitude
2	N_2 2PG (0,0) 337 nm	333.5	341.2	N_2 second positive band filter for observing TLE-s
3	N_2^+ 391.4 nm	387.1	393.6	Proxy for N_2^+ ion production
4	N_2 1PG	608.9	753.4	N_2 first positive band filter
5	OII 777.4 nm	773.6	784.7	Mainly for lightning
6	Broadband MUV	270.0	410.2	Exploratory observations

[a]Note that the band limits are for paraxial rays only. The filter pass-bands are displaced toward the blue for objects lying off axis. In this work, only one of the five, the N_2 first P filter was used in the imager.

[3] The recently launched FORMOSAT-2 (previously known as ROCSAT-2) satellite carries an instrument, the ISUAL, that detects lightning-induced transient luminous events as viewed from orbit in regions above thunderstorms occurring on the Earth limb. Although TLEs have been observed from the space shuttle [*Vaughan et al.*, 1992; *Boeck et al.*, 1992; *Yair et al.*, 2004], ISUAL observations are first in seeing TLEs from space on board a free-flying satellite. In this paper we will briefly describe the ISUAL experiment and a single set of measurements that were taken of elves where the parent lightning was hidden by the Earth limb. By comparing the intensity of the various emissions measured by the photometer, we can estimate the parameters that best describe the electron energy distribution function. From this function we can estimate the ratio between the 391.4 nm measurement and the total ionization produced and thus obtain the number of ionospheric electrons produced by elves.

2. ISUAL Imager and Photometer

[4] The Imager of Sprites and Upper Atmospheric Lightning (ISUAL) is a scientific instrument on the Taiwanese FORMOSAT-2, launched on 20 May 2004. FORMOSAT-2 is in an 891 km altitude Sun-synchronous orbit of 98.99° (81.01° retrograde) inclination. The track of the limb-viewing region of the ISUAL instrument is approximately at midnight local time. Besides being Sun-synchronous, the orbit is also a repeating orbit and the satellite passes over the same geographic location every solar day. This is accomplished by making the orbit period exactly one-fourteenth of the 24-hour day.

[5] ISUAL is the first multiwavelength, quantitative observatory on a free-flying satellite dedicated primarily to observing TLEs. The ISUAL payload includes a visible light intensified CCD imager with a six position filter wheel, a bore-sighted six wavelength channel spectrophotometer (SP), and a two channel array photometer (AP) with 16 vertically spaced, parallel, horizontal strip photomultiplier anodes. The imager is equipped with five selectable filters on a filter wheel and the sixth filter position is open. The SP six filter channel bandpasses range from the far ultraviolet to the near-infrared regions (Table 1). The two AP channels are fitted with broadband filters, one blue and one red. The orbiting nature of the satellite will facilitate the first comprehensive global latitude and longitude survey of TLEs near the midnight local time region. The negligible obscuration of the intervening atmosphere between TLEs and the observer is an additional advantage of space-borne observations. Thus the ISUAL SP provides, for the first time, intensity calibrated emission intensities of sprites and elves, which was problematic to obtain from the ground.

[6] In the selection of the SP filters, two channels (1 and 6) were dedicated to observing the far ultraviolet and midultraviolet wavelength regions, respectively. The other channels were intended for the measurement of relatively well known emissions of the neutral and ionized nitrogen that are significant in TLEs. The preliminary data showed that the ratio of various emissions is highly variable during lightning and the associated TLEs.

[7] The high time resolution requirements for TLE studies produce very high data volumes that would be beyond the capacity of the FORMOSAT-2 satellite data storage and down link transmission systems. To overcome this difficulty, the ISUAL data system operates essentially in a burst mode. Data are gathered continuously during the night pass, but they are saved only if the onboard hardware control system determines that a significant "trigger" event took place. The rest of the data is discarded. For a "trigger" event detection, signals are used from the SP channels and compared to preprogrammable threshold levels in various logical combination. It is difficult to distinguish very bright lightning from TLEs by thresholding. In addition, energetic particles from penetrating radiation in space can provide false signals in the phototubes that are indistinguishable from optically induced events. The satellite has a flexible programmable logic system that can accommodate various "trigger algorithms" and execute them in "real time." The fine tuning of the system is an ongoing process. At the time of writing of this work we have been able to capture about 580 elves and 70 sprites from 8000 lightning events. It should be noted that only the brighter events trigger the system, and therefore this sample is restricted to only those events.

[8] To convert the SP signals that are sensed by photometer channels to the total emissions produced by major molecular bands, we used the preflight calibration and summed the theoretically derived band components intensities multiplied by the wavelength responsivity profile of each photometer channel. The responsivity maximum in

Table 2. Table of Molecular Band Contributions Into Each ISUAL Photometer Channel[a]

	N_2 1P	N_2 2P	N_2 LBH	N_2^+ Meinel	N_2^+1NG
Filter 1	-	-	38.%[a] 17%[b] 3%[c]		-
Filter 2	-	27.80%	-	-	0.80%
Filter 3	-	-	-	-	66%
Filter 4	11%	-	-	4.60%	-
Filter 5	2.6%	-	-	-	-
Filter 6	-	84%	-	-	37%

[a]No O_2 attenuation.
[b]O_2 attenuation when TLE is at 90 km attitude at the viewer side of the terminator.
[c]O_2 attenuation when TLE is at 90 km but at the opposite side of the terminator in both cases the tangent height of the view ray is at 50 km.

each channel was set to unity because the absolute responsivity calibrations (photometer counts per incident photon flux) were also obtained at the response peak of each channel. We have adopted *Vallance Jones* [1974] intensities for N_2 molecular band components. Although the Vallance Jones calculation are only applicable to aurora, and that has generally higher electron energies than TLEs, we assumed that with the relatively low wavelength resolution of the ISUAL SP, the differences in the vibrational distribution or the rotational temperature between TLEs and aurora would be negligible. The fractional contribution of each molecular band of unit intensity for each SP channels is shown in Table 2.

[9] In Table 2, filter 1, some of the LBH calculations included the O_2 absorption as well as the filter response. The O_2 absorption was calculated to 90 km altitude and the O_2 cross sections were calculated using polynomial coefficients [*Minschwaner et al.*, 1992] including the Herzberg continuum cross section in the range in the wavelength of interest [*Yoshino et al.*, 1988]. The O_2 absorption depends on the total O_2 column between the TLE and the observer therefore on the angle of view. In Table 2 we assumed a view geometry where the tangent height of the ray viewing the cloud is 50 km above the Earth surface. We included both when the cloud is this side of the limb (case 2) and when on the other side (case 3). In the interpretation of LBH intensities the O_2 absorption has to be evaluated on a case-by-case basis.

[10] The degree that LBH is emitted depends on the lifetime of the LBH upper state, the $a^1\Pi_g$ state whose life time is was measured in laboratory experiments by several groups [*Holland*, 1969; *Shemansky*, 1969; *Pilling et al.*, 1971]. The most recent and probably the most accurate measurement is that of *Mason* [1990] showing that the lifetime of the N_2 $a^1\Pi_g$ state is 120 ± 20 μs. The quenching coefficient for N_2 ($a^1\Pi_g$, $v' = 0$) is given as $<3 \times 10^{-10}$ by *Vallance Jones* [1974] but more recent two-photon laser excitation measurements show it to be 2.2×10^{-11} $cm^3 s^{-1}$ [*Marinelli et al.*, 1989]. From this the quenching height is lowered to 70 km and quenching is likely to be less important in elves than in sprites or other lower-altitude TLEs. Channel 1 is useful in that it sees TLE emissions produced only above the ozone layer (30 km), and therefore it is blind to tropospheric lightning.

[11] A good recent reference for space-based observations of auroral emissions that may be relevant to the UV channels 1 and 2 and that have not been included in Table 2 is a relatively recent auroral spectra taken by the Mid-course Space Experiment (MSX) satellite [*Strickland et al.*, 2001]. ISUAL channels 1 and 2 would pass the prominent auroral emission feature near 214.5 nm [*Dick*, 1978], which was thought to be one of the doublet lines (213.968 and 214.355 nm) emitted by metastable N^+ (^5S) ions. Dissociative excitation of N_2 by electron impact with a cross section greater than or equal to 2×10^{-18} cm^2 has been proposed as the source of this species. Detailed laboratory study of *Erdman et al.* [1980] questioned this mechanism and it is difficult to predict its importance in TLEs. The 247 nm OII and 297.2 nm OI emissions have relatively long lifetimes and require the presence of atomic oxygen at the production altitude. Likewise, the lifetime of the upper state of the Vegard-Kaplan is also too long to produce significant emission below 100 km.

[12] The second filter passes the N_2 2P (0, 0) band and Table 2 shows that 27.8% of the entire band system is within this filter band. The third filter was designed for the measurement of the N_2^+ first negative (0, 0) band, and it contains 66% of the entire band. The filter band is wide enough to contain all branches of the 0, 0 band regardless of temperature. The excitation cross section for producing the upper state of this by electron impact has been measured by *Borst and Zipf* [1970]. They showed that the ratio of the total ionization cross section to this excitation cross section was nearly constant over the energy range from 30 eV to 10 keV, and has a value of 14.1. In aurora where the high-energy electrons are dominant this applies and the measurement of the 391.4 nm emission of the N_2^+ first negative (0, 0) can be quantitatively related to the total ion production. Although the presence of this emission is a qualitative proof of local ion production, we cannot use the fixed ratio for TLEs unless we can show that there are no significant electron fluxes in the less than 30 eV range.

[13] Filter 4 is responsive to the N_2 first positive and N_2^+ Meinel bands with 11 and 4.6% contribution into each, respectively. This filter was chosen because these bands were the most intense contributors in sprites and elves from ground-based measurements [*Mende et al.*, 1995; *Hampton et al.*, 1996]. Filter 5 is for the OI 777.4 nm, which is the choice wavelength for monitoring lightning from space [*Christian et al.*, 2003]. Photometer channel 6 covers the broad band in the middle UV with substantial input from the N_2 2P and N_2^+ first negative bands.

3. Interpretation of Optical Measurements

[14] For optical transitions where collisional quenching is negligible the lifetime of the *k*th state is $\tau_k = 1/A_k$, where A_k is the Einstein coefficient. If the pulse duration of the excitation Δt is also much longer than τ_k, then the emission rate is simply

$$I_k = 10^{-6} \int_0^\infty \upsilon_k \, N_e \, dl \text{ (Rayleighs)}, \qquad (1)$$

where υ_k is the excitation rate, N_e is the electron density, and dl is a length increment along the line of sight. The total

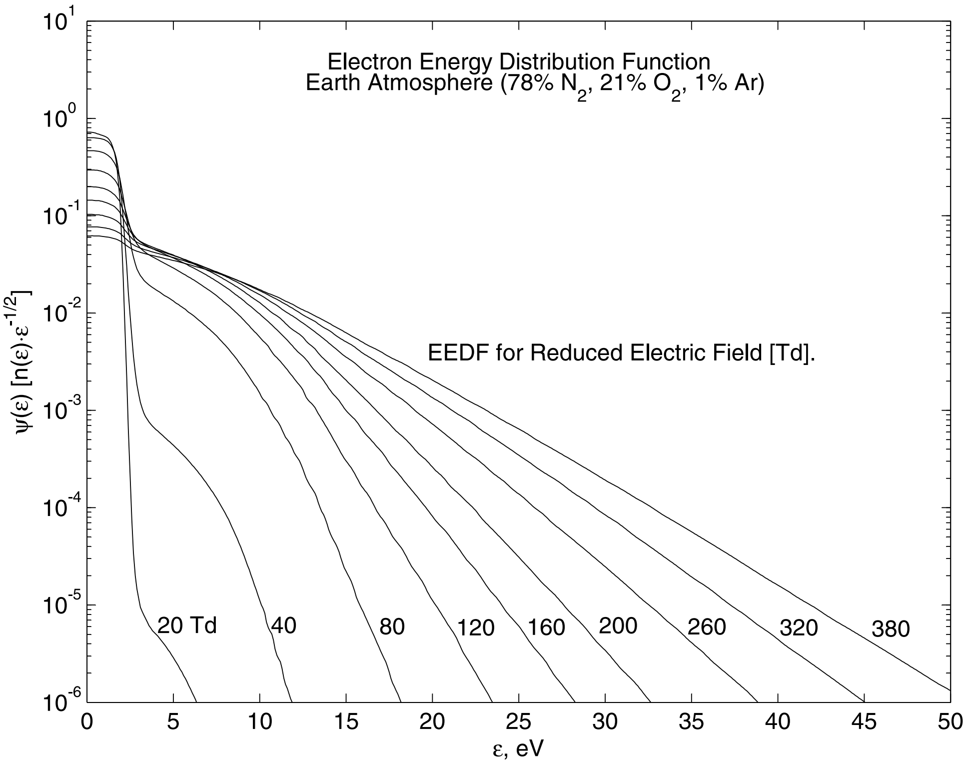

Figure 1. Electron energy distribution for reduced electric fields of 20 to 380 Townsend.

integrated luminous flux produced in the pulse of Δt duration are

$$P_k = \Delta t\ 10^{-6} \int_0^\infty \upsilon_k\ N_e\ dl\ \text{(Rayleigh seconds)}. \quad (2)$$

In order to predict the relative intensities of the various emissions that we can measure with ISUAL, we need to evaluate υ_k for the parent states that contribute to emissions observed by ISUAL.

$$\upsilon_k = N_e \int_0^\infty \sigma_k\, v\, n_e(E) dE, \quad (3)$$

where σ_k is the total excitation cross section from ground state to the kth state, $v = \sqrt{2E/m_e}$ is the electron velocity, and $n_e(E)$ is the electron energy distribution function. Thus

$$\upsilon_k = N_e \sqrt{(2/m_e)} \int_0^\infty \sigma_k \sqrt{(E)} n_e(E) dE. \quad (4)$$

[15] The electron density distribution function is usually evaluated by solving the Boltzmann equation [e.g., *Taranenko et al.*, 1993a, 1993b]. The solutions depend on the electronic reaction properties of the atmospheric constituents and the result is the electron energy distribution function $n_e(E)$ as a function of E, the locally applied TLE reduced electric field. The solutions are independent of the altitude if the applied electric field is expressed as the reduced electric field namely the electric field divided by pressure (or density). We use the unit Townsend (Td) for the reduced electric field, where 1 Townsend = 1×10^{-21} V m^2 = 1×10^{-17} V cm^2 [*Raizer*, 1997]. The resultant electron energy distribution function is shown in Figure 1. Several others [e.g., *Taranenko et al.*, 1993a, 1993b; *Pasko et al.*, 1997; *Hiraki et al.*, 2004] performed such calculations.

[16] We have evaluated equation (4) numerically for several spectral bands using the electron density distribution of Figure 1 and the applicable cross sections. Using the cross sections tabulated by *Phelps and Pitchford* [1985] and by *Phelps* [1991], we have obtained the theoretically expected excitation coefficients, υ_k for the N_2 ($B^3\Pi$) upper state of the N_2 first positive band (BVJ), for the N_2 ($C^3\ \Pi$) of the N_2 second positive (337.1 nm), for the N_2^+ ($B^2\Sigma_u^+$) upper state of N_2^+ first negative (0, 0) band (391.4 nm), for the N_2 ($a^1\Pi$) of LBH and the production rate for N_2^+ ions (total ionization). The notation BVJ was used because the excitation coefficients for the B state as used here include cascades from other states in a manner similar to their usage by *Vallance Jones* [1974]. All the calculations assume that the excitation or ionization is from the electronic ground state and impact excitation from excited states is neglected. The BVJ excitation rate includes cascade contributions only from N_2 ($C^3\Pi$) state. The 337.1 nm rates were computed using the excitation rate of N_2 ($C^3\Pi$) and then applying the Franck-Condon factor of 0.545 for the (C-B) 0–0 transition taken from *Gilmore et al.* [1992]. The 391.4 nm emission rates are computed using the excitation rate of N_2^+ ($B^2\Sigma_u^+$) from the ground state of N_2 and then applying the Franck-Condon factor of

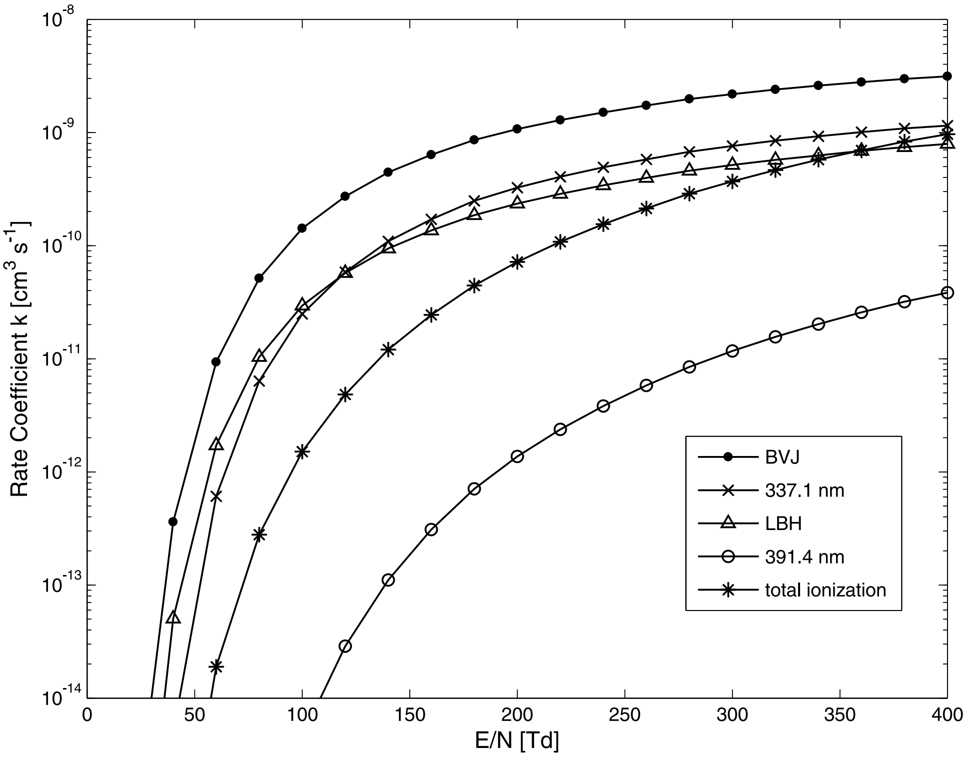

Figure 2. Excitation coefficients as calculated from the electron energy distribution function for the N_2 ($B^3\Pi$)) including cascades from the B states, a treatment similar to *Vallance Jones* [1974] (BVJ), N_2 ($C^3\Pi$)) (337.1 nm), the N_2 ($a^1\Pi$)) state (LBH), N_2^+ ($B^2\Sigma_u^+$) (391.4 nm), and the total ion production rate.

0.883 for the transition 0, 0 transition [*Gilmore et al.*, 1992]. The total ionization shown includes N_2 ionization into the N_2^+ X, A, and B states, as well as O_2 direct ionization. The calculations were completed prior to the recent publication of new cross sections by *Shemansky and Liu* [2005]. The results are therefore based on cross sections that were available previously and might be subject to (hopefully) minor corrections.

[17] Dissociative ionization, namely molecular dissociation resulting in N^+ ions, is not included here, although in aurora that might be a significant (30%) contributor of nitrogen ions [e.g., *Prassad and Green*, 1971] or the more recent work of *Lindsay and Mangan* [2003]. Since this process requires high-electron energy, the process is more likely to be important in aurora where higher-energy electrons are available. Again from energy considerations, dissociative ionization of O_2 is much less likely to happen than direct ionization of molecular O_2. At the altitude of elves ~90 km the O concentration is still low compared to O_2. The ionization contribution from atomic O was also neglected. The results are shown in Figure 2. It should be noted that all these features have negligible quenching at the elves altitude region 80 km and above.

[18] By comparing ratios, we can eliminate the unknown initial ambient electron density, and therefore we can compare the measured ratios directly with the theoretical ones. In Figure 3 the theoretical ratios between the various estimated features and the N_2 second positive is plotted. Although the N_2 first positive has the advantage that most ground-based optical observations use this feature, we used the second positive as our base line because (1) the lifetime of the second positive is very short at all altitudes in the TLE range, (2) the entire 0, 0 component (27% of the whole band) is unambiguously measured by channel 2 of the ISUAL SP, and (3) there are no questions related to the possible presence of contributions due to cascading from other states.

4. Measurements

[19] During the first few months of operation, ISUAL was "triggered" by 8000 lightning events, and as many as 580 of these events were accompanied by some elves luminosity. Unfortunately, as we have indicated earlier, the "trigger" criteria of the instrument is not well enough characterized yet to define the precise conditions under which an event is counted by ISUAL. Thus it is still hard to draw significant statistical conclusion except that observable elves are a frequent perturbation of the mesosphere and they accompany between 5 and 10% of the larger lightning flashes.

[20] The fields of view of the SP and the imager are essentially the same and the imager monitors the spatial distribution of the visible light output in the field of view of the SP. When observing TLEs downward from a spacecraft, it is mostly impossible to avoid seeing the lightning below the TLE. Thus most SP observations of TLEs have significant contamination from the associated lightning and careful analysis is needed to distinguish the TLE induced signal from lightning. Fortunately, there were a few events that were located so that the associated lightning was over the horizon and was obscured by the solid Earth limb while

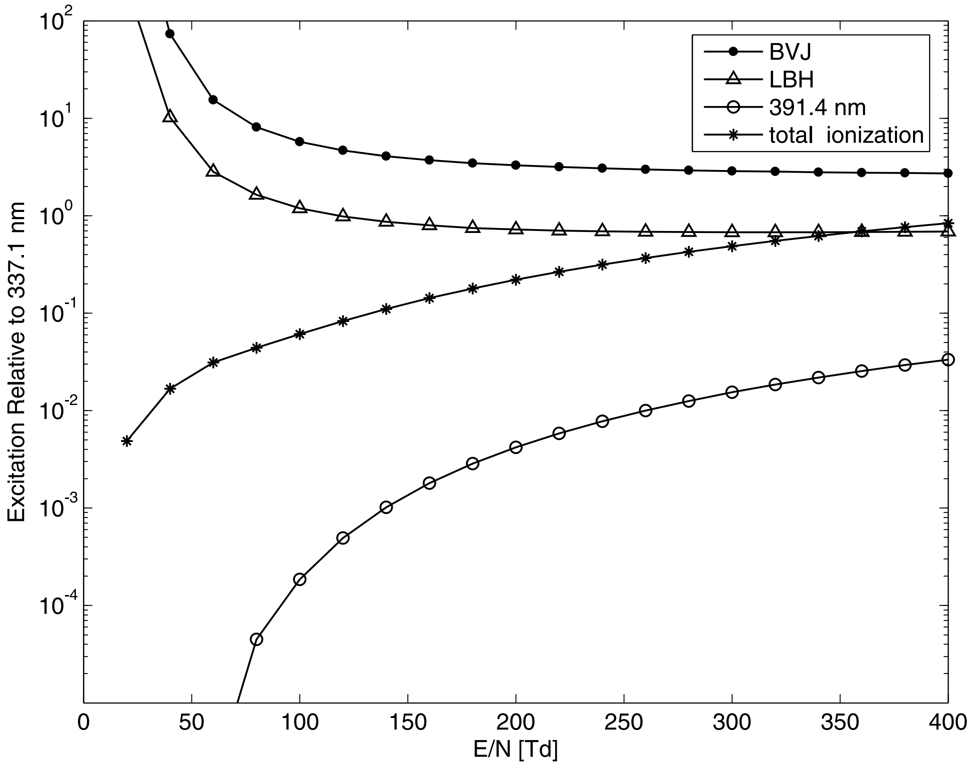

Figure 3. Excitation coefficient ratios of the N_2 emission features and the N_2 second positive emission. The legend shows the associated emission ratio with each curve. BVJ is the curve representing the ratio of the first positive emission.

the TLE above was in full view of ISUAL. Such an event was observed on 7 August 2004. Three image frames of this event are shown on Figure 4 and the corresponding SP traces are presented in Figure 5.

[21] The brightnesses appear to be very large (e.g., 6 MR in the N_2 first positive band). However, the total energy in the pulse is quite modest since it lasts only for $<10^{-3}$ s and the entire pulse is equivalent to light produced in a relatively weak aurora of 3.28 kR intensity during 1 s.

[22] From these measurements we can obtain the total number of photons created by the elves by integrating the light pulse for the duration of the elves to compare with equation (2) and the peak production rates by measuring the peak intensity of the pulses (equation (1)).

[23] In Table 3 we show the quantities derived from the measurement of the time integrated counts of the light pulse in each photometer channel. This allows the estimation of the total number of photon produced by the elves in each excited state. The SP was calibrated in the laboratory with a known intensity light source, which subtended a known solid angle to the source. In Table 3 the photometer signals were shown due to the elves (after the subtraction of a stable background level). Using the calibration data, we converted the photometer data to photon flux reaching the photometers expressed in photons cm^{-2} falling on the photometer front lens during the pulse (column 2). Column 3 is the flux converted into Rayleigh seconds recognizing that the SP counting interval is 0.0001 s (one Rayleigh is equivalent to $10^6/4\pi$) photons $sterad^{-1}$ s^{-1} cm^{-2}. The apparent brightness, flux-emitted per cm^2 of the elves can be estimated from photon flux and the area of the luminous region of the elves image. To proceed, we assumed that the spatial distribution of the elves luminosity was the same in all the wavelength channels of the SP as in the N_2 first positive band image taken by the imager. From this assumption, we can then establish the number of pixels that were lit up by the elves and the solid angle subtended by the elves. To translate the elves angular size to actual linear distances, the range distance to the elves was needed. From the geometry of the observation with the satellite altitude (891 km), the tangent height of the OH airglow (87 km), the approximate altitude of the elves ($\sim$90 km), and the measured angular difference between the airglow and the elves, we were able to estimate that the range distance to the elves from the satellite was about 4000 km. On the basis of this range estimate and on the imager pixel count, the diameter of the elves was about 165 km. From the photon flux incident on the photometer, we were able to estimate the time integrated number of photons emitted in each wavelength band by the elves. By dividing by the horizontal area ($165^2\pi$)/4 km^2) of the elves, we obtained the time integrated brightness in Rayleigh s when viewing the circular brightness region associated with the elves from below (third column). In column 4 we showed the percentage contribution of the various selected bands in each filter (Data from Table 2). Column 5 is the derived total band intensity in Rayleigh seconds as obtained from column 3 and 4. Column 5 is the ratio of the derived time integrated total band intensity (Column 4) to the derived N_2 second positive intensity of channel 2.

[24] The total luminous energy produced, P_k in the pulse of duration Δt can be expressed as a line of sight integral of

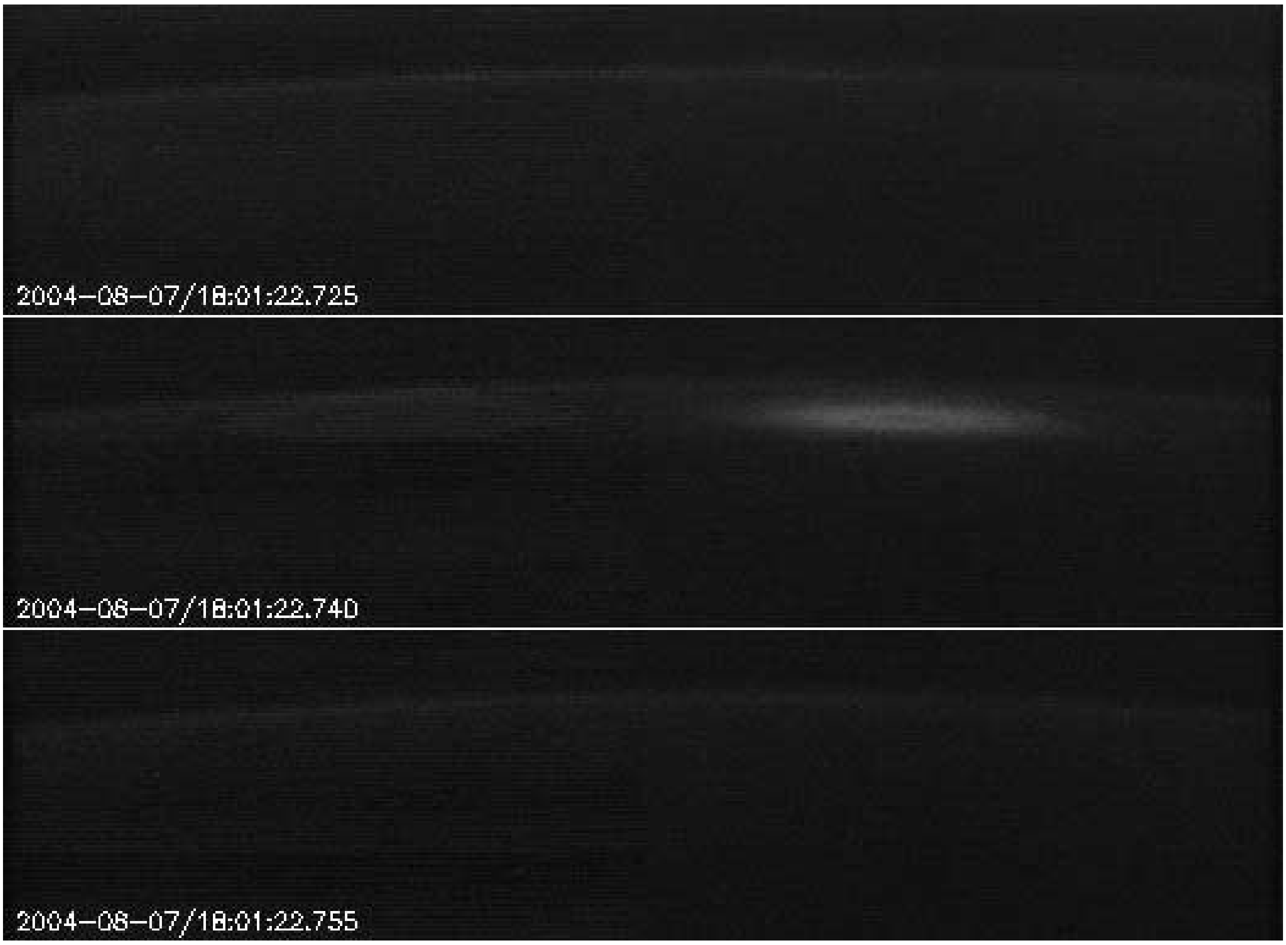

Figure 4. Elves event on 2004-08-07 at 1801:22. Top field is the field prior to the "trigger" and the bottom field immediately following it. The image in the middle shows the elves as a donut-shaped object, this luminosity distribution is in agreement with the predictions of *Inan et al.* [1997].

terms of υ_k and N_e (equation (2)). In order to obtain the average υ_k along the line of sight, the integral of equation (2) needs to be divided by the length of the TLE luminosity along the line of sight. If we assume that the TLE is viewed from below, then we need to assume a vertical layer thickness to calculate the true volume emission rate. We assumed that the vertical distance is 10 km (1×10^6 cm) which cancels with the 1×10^6 photons emitted in 4 π steradian when converting it to volume emission in photons cm^{-3} (column 7).

[25] In Table 4 the peak brightness measurements were tabulated for each channel for the event. The peak rates were obtained from the SP calibrations and by scaling the counts by the SP counting interval duration of 0.1 ms. Using similar considerations regarding the spatial extent of the elves as in Table 3, we included the observed temporal intensity peak of the photon flux at the photometer lens (photons cm^{-2} s^{-1}, column 2), the spatially averaged intensity (MRayleighs, column 3) as viewed obliquely by the photometer, the derived total intensity produced by the entire band system (Rayleighs, column 4). Filter 4 is mostly sensitive to the N_2 first pos band and we find that the estimated band peak intensity is 44 MR (column 4). Theoretically predicted number for this intensity is >10 MR [*Inan et al.*, 1996] and the predictions have been verified by ground-based measurements [*Barrington-Leigh and Inan*, 1999].

[26] The absolutely calibrated ISUAL imager observed the same feature with its N_2 first pos band filter. To check the consistency of the imager and SP calibrations, we compared the two. The imager was used in a mode where the exposure duration was 14 ms and the elves duration was shorter we can only make an integrated luminosity measurement of the elves with the imager. According to the imager calibration, the sensitivity of the imager at this time was 36.1 counts per MR at the appropriate microchannel plate gain and exposure duration. The analysis of the image showed that the average brightness was $\sim$12 counts per pixel giving 332 kR. This is equivalent to 3.7×10^8 photons $sterad^{-1}$ cm^{-2} for an exposure time of 14 ms and since the cloud subtended a solid angle of 6.88×10^{-4} the total light on the imager optics were 2.5×10^5 photons cm^{-2}. From the prior discussion, filter 4 (Table 3, column 2) showed that the total number of photons that fell on the SP aperture was 1.8×10^5 photons cm^{-2}. Comparing this with the imager measurement of 2.5×10^5, this can be considered as fair

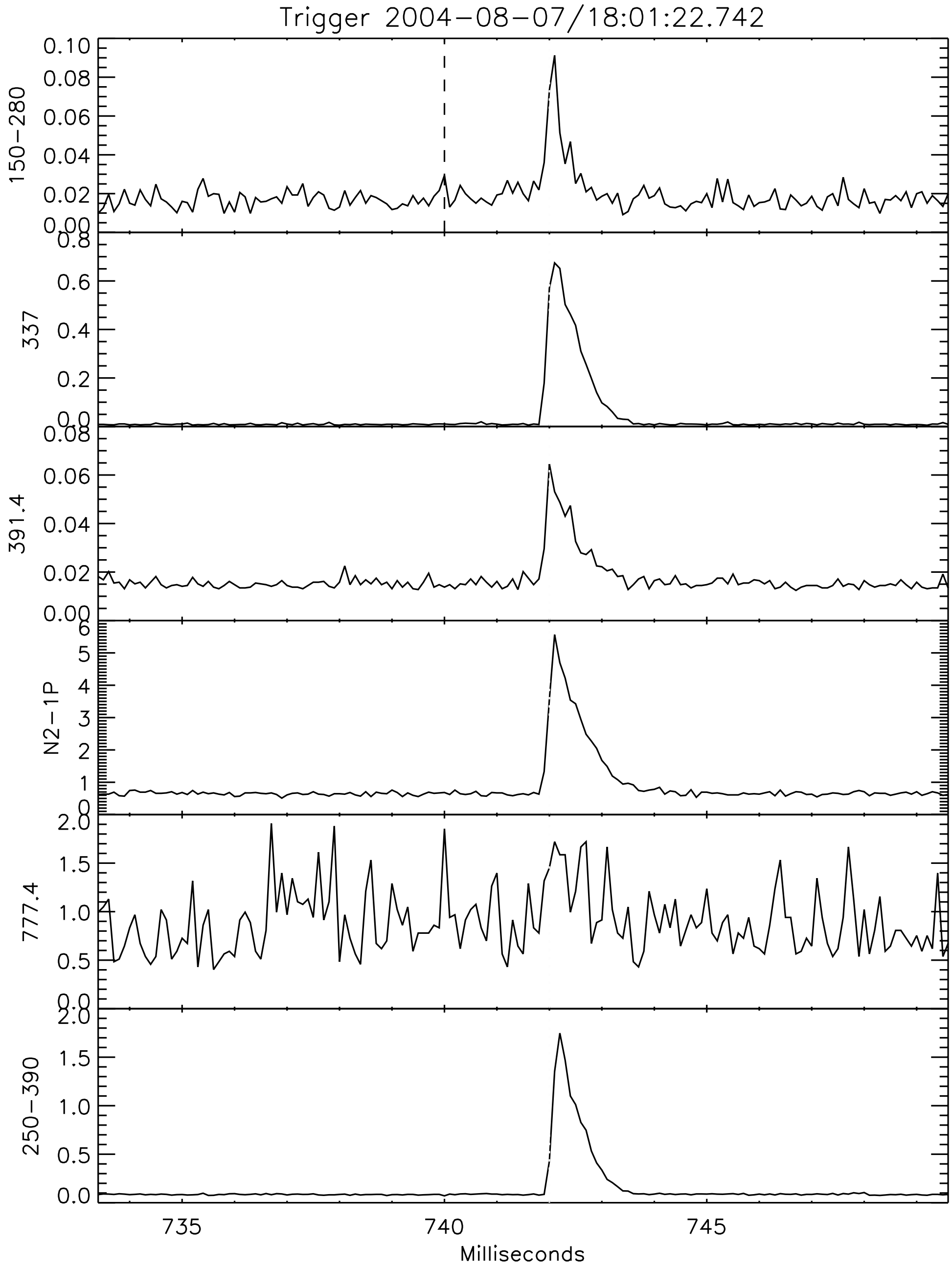

Figure 5. The photometer traces for the event 2004-08-07 at 1801:22, presented in Figure 4. The ordinates are labeled in MRayleighs averaged over the spatial extent of the elves in the image (Figure 4). Channels are in sequence from 1 to 6 (Table 1) and the approximate wavelength ranges associated with each channel are noted on the left. N_2-1P represents the broadband filter of Channel 4. The x axis is labeled in ms.

agreement (±25%). Some of the inaccuracies can be attributed to temperature changes between calibration and on orbit operations.

5. Interpretations

[27] The 391.4 nm signal in channel 3 is produced by the permitted transition from N_2^+ ($B^2\Sigma_u^+$) state and the presence of this emission shows that ion production definitely does occur. Quantitatively, the ratio of the total ionization cross section to that of the excitation of 391.4 nm is a constant (14.1) [*Borst and Zipf*, 1970] for higher-energy electrons and in fact it is a good approximation in aurora. This is illustrated in Figure 2 where we plotted the total ionization and the 391.4 nm excitation. According to the measurements (Table 3 column 6) the ratio of emission 391.4 nm to the N_2 second positive is 0.026. The theoretically derived ratios of Figure 3 show that the ratio is 2×10^{-4} for 100 Td rising to 0.03 at 400 Td. The measured 0.026 implies high values of reduced electric fields.

[28] On the basis of the above we can conclude that the reduced electric field in the elves was high >200 Td. From

Table 3. Time-Integrated Intensities and Yields in the Pulse

Photometer Channels	Time-Integrated Photons at Photometer, cm^{-2}	Vertical Column Intensity, 10^6 photons cm^{-2}	Ratio to Band Total From Table 2	Total Band Column Intensity, 10^6 photons cm^{-2}	Ratio of the Measured Intensity to N_2 Second Positive	Time-Integrated Production Rate, cm^{-3}, Assuming 10 km Layer Thickness
Filter 1	1521	14	2.40%[a]	594	~0.7	594
Filter 2	24,956	234	27.8%	842	1	842
Filter 3	1609	15	100%[b]	23	0.026	23
Filter 4	182,288	1709	11%	15535	18.4	15535
Filter 5	0	0	100%	0	0.0000	0
Filter 6	52,114	489	84%	582	0.69	582

[a]O_2 absorption 90 km TLE height 50 km tangent height of view axis.
[b]Applying to the 391.4 nm (0, 0) feature of the N_2^+ first negative band.

Figure 2 the ratio of the ionization production rate to 391.4 nm is close to the constant value characteristic of high reduced electric field values. Since the total spatially averaged production of 391.4 nm in the elves was of 23 photons cm^{-3} (table 3, column 7, row 3), we find that the average ion production in the elves was about 210 ions cm^{-3} for an event that was 10 km thick in altitude. The theoretically predicted ratio of the intensity of the N_2 first positive to the N_2 second positive is also shown on Figure 3 as curve labeled BVJ. This ratio goes from 100 at 40 Td to about 3 at 400 Td. The measured ratio was about 18.4 (Table 3, column 6, filter 4). According to Figure 3, this ratio would signify a lower value of reduced electric field in the neighborhood of 50 Td. To make this measurement more consistent with the other measurements, we would need to have a smaller ratio, e.g., 4 or 5. Note that the theoretical ratios of Figure 3 do not include all the cascading terms in the N_2 first positive emission ratio. Had those been included the predicted ratio would have been larger and better agreement could have been found.

[29] These were the first space-based measurement of elves uncontaminated by lightning and were only minimally modified by atmospheric absorption for most features. In discussing the N_2 LBH emissions, however, we still needed to estimate the significant O_2 absorption from the total integrated O_2 density along the line of sight. This can be calculated by the following expression:

$$L = \int_{h_t}^{h_p} 2\ N\ (h)\left(1 - ((h_t + R_E)/(h + R_E))^2\right)^{-1/2}\ dh + \int_{h_p}^{h_s} N\ (h)\left(1 - ((h_t + R_E)/(h + R_E))^2\right)^{-1/2}\ dh, \qquad (5)$$

where h_t is the tangent height of the ray to the observed phenomena, h_p is the altitude of the phenomena, h_s is the altitude of the satellite, $N(h)$ is the number density of the absorbing species as a function of height (h), R_E is the Earth radius, and h is the altitude variable. Equation (5) applies to observations that are looking at the phenomena on the other side of the solid Earth terminator. If the TLE is on the same side of the terminator as the observer, then only the second term in equation (5) is used. From the image of a TLE it is possible to measure the tangent height of the ray to the TLE by determining the number of pixels between the airglow upper boundary and the center of the TLE. From the altitude of the airglow layer terminator (85–90 km), the satellite altitude (891 km), and the measured pixels converted into angle, the tangent height of the rays to the TLE can be obtained. From these considerations we found the tangent height of the ray to the center of the TLE was about 50 km. The value of expression (equation (5)) is more dependent on the tangent height of the ray, h_t than on the altitude of the TLE, h_p. Assuming that the TLE height was 90 km, from equation (5) we find that the column integrated O_2 density between the TLE and the satellite was 2.09×10^{23} cm^{-2} compared to 7.5×10^{18} cm^{-2} for direct downward viewing to 90 km. The O_2 Schumann-Runge region in the ultraviolet is a very effective absorber of LBH. Note that the column densities given here are only equivalent to only about a 400-m long air column at ground level. Thus in the ISUAL observation, the atmospheric extinction can be neglected in most wavelength regions except in the far ultraviolet.

[30] We interpret that SP channel 1, the far ultraviolet channel, is mostly sensitive to LBH. In a qualitative sense this is consistent with observations, namely the lack of response from terrestrial lightning and the large variability of the signal from TLEs such as sprites and elves. From the theoretical curves (Figure 3) of the ratios of the excitation coefficient of the N_2 ($a^1\Pi$) state (LBH) and N_2 ($C^3\Pi$) state (the N_2 second pos) should be < 1.0 for E/N range of >100 Td. The measured ratio in Table 3 column 6 is ~0.7, consistent with E/N greater than 100 Td. As we have mentioned, the LBH band is strongly absorbed by atmospheric O_2 and the above obtained value depends on the column density of O_2 (2.09×10^{23} cm^{-2}) along the line of

Table 4. Peak Intensity and Corresponding Rates

	Photon Flux, 10^6 cm^{-2} s^{-1}	Spatially Averaged Intensity, M Rayleighs	Total Band Intensity, M Rayleighs
Filter 1	31	0.0723	3.01
Filter 2	288	0.6638	2.39
Filter 3	21	0.0494	0.075
Filter 4	2134	4.9176	44.7
Filter 5			0
Filter 6	721	1.6613	1.97

sight between the elves and the satellite. In addition the laboratory calibration of channel 1 is somewhat in question because no direct calibration data was obtained with the high voltage value that was actually used in the measurement. The measured value is based on an extrapolation of the gain behavior of the channel 1 photo multiplier tube.

6. Discussion

[31] We have obtained that the spatially averaged number of electrons produced by the elves was 210 electrons cm^{-3} for a horizontal layer of an assumed 10 km vertical thickness. The photometer measurements more directly represent the total photon production by the elves as a whole. The 391.4 nm channel measured 1609 photons cm^{-2} (Table 3, column 2). These were seen by the photometer at a radial distance of 4000 km thus 3.23×10^{21} photons were produced in total by the elves event. This is equivalent to an electron enhancement of 4.5×10^{22} electrons or an increase in the vertical column density of 1.5×10^{7} electrons cm^{-2}.

[32] It might be interesting to compare the 210 electrons cm^{-3} electron density increase to what is the expected ambient ionospheric density. From the IRI model using the appropriate day 7 August 2004 midlatitude, midnight local time, and an ionospheric-effective solar index IG12 of 45.4 we find that the nighttime electron density profile rises rapidly from 2 electrons cm^{-3} at 80 km altitude to $\sim$500 e cm^{-3} at 90 km. Therefore under conditions where the ambient nighttime *D* region electron density is low, lightning EMP is sufficiently strong to excite optical emissions in the form of elves and would appear to constitute a local source of ionization in the upper atmosphere. Observable elves occur during >5% of the most intense lightning flashes. Although the frequency of such flashes or indeed that of the elves is hard to estimate from the currently available data, the electron production is quite extensive covering an area of several hundred square kilometers.

[33] To compute the ionization, we have obtained the reduced electric field in the elves and found that it was of the order of 200 Td. This appears higher than expected, however, assuming that the sprite is at an altitude of 90 km this field is equivalent to an electric field of 7.8 V m^{-1}. We can be reasonably confident that the electric field is generated by an EMP originating in the lower atmosphere, and therefore the field will scale as an inverse function of the radial distance from the source. Assuming that the lightning occurred at 1 km above ground directly underneath the elves, the electric field measurements would scale to 10 V m^{-1} at 70 km and 36 Vm^{-1} at 20 km. In other words, the field in the lower atmosphere is relatively small and inadequate to produce spontaneous breakdown of any kind.

[34] These ISUAL measurements are the first absolute intensity ratio measurements that are largely unobstructed by uncertain atmospheric conditions. These measurements therefore are the first true tests of the theoretical modeling predictions of expected TLE luminous brightness that abound in the literature.

7. Summary

[35] The spectrophotometer (SP) and the imager of the ISUAL instrument on FORMOSAT-2 fortuitously observed elves in such a way that the associated lightning was hidden by the Earth's limb. Analysis of the measured luminosity showed that the elves produced all the well-known bands of atmospheric nitrogen including the LBH bands in the far ultraviolet, the N_2 second positive in the middle ultraviolet, and the first positive band in the visible/IR. The observations showed significant intensity of N_2^+ first negative (0, 0) band. The measured emission intensities were more or less consistent with theoretical expectation for the ratios of the LBH and the N_2^+ first negative to the N_2 second positive. From these ratios we have obtained an approximate value for the reduced electric field responsible for the elves discharge, and it was found to be quite high, >200 Td. Using the electric field estimates allowed us to express the ratio of the total ionization to the N_2^+ first negative emission and we found that the ion yield averaged for the elves geometry was about 210 cm^{-3} over the elves that covered several hundred square kilometers.

[36] **Acknowledgments.** The Imager of Sprites and Upper Atmospheric Lightning was a collaborative effort between, the National Chen Kung University of Taiwan, the University of California, Berkeley (UCB), Tohoku University of Japan and the National Space Program Office of Taiwan. The authors are indebted to the technical staff at each of these institutions. Special mention is made of You-Shin Chang of NSPO and Henry Heetderks and Stewart Harris of UCB, who as program managers made outstanding contributions to the program. This project was funded by the NSPO of Taiwan.

[37] Arthur Richmond thanks Donald E. Shemansky and another reviewer for their assistance in evaluating this paper.

References

Barrington-Leigh, C. P., and U. S. Inan (1999), Elves triggered by positive and negative lightning discharges, *Geophys. Res. Lett.*, *26*, 683–686.

Boeck, W. L., O. H. Vaughan Jr., R. Blakeslee, B. Vonnegut, and M. Brook (1992), Lightning induced brightening in the airglow layer, *Geophys. Res. Lett.*, *19*, 99–102.

Borst, W. L., and E. C. Zipf (1970), Cross section for electron-impact excitation of the (0, 0) first negative band of N_2^+ from threshold to 3 keV, *Phys. Rev. A*, *1*, 834–840.

Christian, H. J., et al. (2003), Global frequency and distribution of lightning as observed from space by the Optical Transient Detector, *J. Geophys. Res.*, *108*(D1), 4005, doi:10.1029/2002JD002347.

Dick, K. A. (1978), The auroral 2150 A feature: A contribution from lines of singly ionized atomic nitrogen, *Geophys. Res. Lett.*, *5*, 273–274.

Erdman, P. W., P. J. Espy, and E. C. Zipf (1980), A laboratory study of the lambda 2145 A auroral mystery feature, *Geophys. Res. Lett.*, *7*, 761–764.

Fukunishi, H., Y. Takahashi, M. Kubota, K. Skanoli, U. S. Inan, and W. A. Lyons (1996), Elves: Lightning-induced transient luminous events in the lower ionospohere, *Geophys. Res. Lett.*, *23*, 2157–2160.

Gilmore, F. R., R. R. Laher, and P. J. Espy (1992), Franck-Condon factors, centroids, electronic transition moments, and Einstein coefficients for many nitrogen and oxygen band systems, *J. Chem. Ref. Data*, *21*, 1005–1103.

Hampton, D. L., M. J. Heavner, E. M. Wescott, and D. D. Sentman (1996), Optical spectral characteristics of sprites, *Geophys. Res. Lett.*, *23*, 89–92.

Hiraki, Y., L. Tong, H. Fukunishi, K. Nanbu, Y. Kasai, and A. Ichimura (2004), Generation of metastable oxygen atom O (1D) in sprite halos, *Geophys. Res. Lett.*, *31*, L14105, doi:10.1029/2004GL020048.

Holland, R. F. (1969), Excitation of nitrogen by electrons: Lyman-Birge-Hopfield band system of N_2, *J. Chem. Phys.*, *51*, 3940.

Inan, U. S., T. F. Bell, and J. V. Rodriguez (1991), Heating and ionization of the lower ionosphere by lightning, *Geophys. Res. Lett.*, *18*, 705–708.

Inan, U. S., W. A. Sampson, and Y. N. Taranenko (1996), Space-time structure of optical flashes and ionization changes produced by lightning-EMP, *Geophys. Res. Lett.*, *23*, 133.

Inan, U. S., C. Barrington-Leigh, S. Hansen, V. S. Glukhov, T. F. Bell, and R. Rairden (1997), Rapid lateral expansion of optical luminosity in lightning-induced ionospheric flashes referred to as "elves", *Geophys. Res. Lett.*, *24*, 583.

Lindsay, B. G., and M. A. Mangan (2003), Cross sections for ion production by electron collision with molecules, in *Landolt-Bornstein, Photon- and Electron-Interaction Wih Molecules: Ionization and Dissociation*, vol. I/17C, edited by Y. Itikawa, pp. 1–77, Springer, New York.

Marinelli, W. J., W. J. Kessler, B. D. Green, and W. A. M. Blumberg (1989), Quenching of N_2 (a 1Pi sub g, v-prime = 0) by N_2, O_2, CO, CO_2, CH_4, H_2, and Ar, *J. Chem. Phys.*, *90*, 2167–2173.
Mason, N. J. (1990), Measurement of the lifetime of metastable species by electron impact dissociation of molecules, *Meas. Sci. Technol.*, *1*, 596–600.
Mende, S. B., R. L. Rairden, G. R. Swenson, and W. A. Lyons (1995), Sprite spectra; N_2 1 PG band identification, *Geophys. Res. Lett.*, *22*, 2633.
Minschwaner, K., G. P. Anderson, L. A. Hall, and K. Yoshino (1992), Polynomial coefficients for calculating O2 Schumann-Runge cross sections at 0.5/cm resolution, *J. Geophys. Res.*, *97*, 10,103–10,108.
Pasko, V. P., U. S. Inan, and T. F. Bell (1997), Sprites as evidence of vertical gravity wave structures above mesoscale thunderstorms, *Geophys. Res. Lett.*, *24*, 1735.
Phelps, A. V. (1991), Cross Sections and Swarm coefficients for nitrogen ions and neutrals in N_2 and argon ions and neutrals in Ar for energies from 0.1 eV to 10 keV, *J. Phys. Chem. Ref. Data*, *20*, 557–573.
Phelps, A. V., and L. C. Pitchford (1985), Anisotropic scattering of electrons by N_2 and its effects on electron transport: Tabulations of cross sections and results, *JILA Rep. 26*, Joint Inst. for Lab. Astrophys., Univ. of Colo., Boulder, Colo.
Pilling, M. J. A., A. M. Bass, and W. Braun (1971), A curve of growth determination of the f values for the fourth positive band of CO and the Lyman Birge Hopfield band system of N_2, *J. Quant. Spectrosc. Radiat. Transfer*, *11*, 1593.
Prasad, S. S., and A. E. S. Green (1971), Ultraviolet emissions from atomic mitrogen in the aurora, *J. Geophys. Res.*, *76*, 2419–2428.
Raizer, Y. P. (1997), *Gas Discharge Physics*, 449 pp., Springer, New York.
Rowland, H. L., R. F. Fernsler, J. D. Huba, and P. A. Bernhardt (1995), Lightning driven EMP in the upper atmosphere, *Geophys. Res. Lett.*, *22*, 361–364.
Shemansky, D. E. (1969), N_2 Lyman-Birge-Hopfield band system, *J. Chem. Phys.*, *51*, 5487.
Shemansky, D. E., and X. Liu (2005), Evaluation of electron impact excitation of N_2 $X^1\Sigma_g^+(0)$ into the N_2^+ $X^2\Sigma_g^+$ (v), $A^2\Pi_u$(v) and $B^2\Sigma_u^+$(v) states, *J. Geophys. Res.*, *110*, A07307, doi:10.1029/2005JA011062.
Strickland, D. J., J. Bishop, J. S. Evans, T. Majeed, R. J. Cox, D. Morrison, G. J. Romick, J. F. Carbary, L. J. Paxton, and C.-I. Meng (2001), Midcourse space experiment/ultraviolet and visible imaging and spectrographic imaging limb observations of combined proton/hydrogen/electron aurora, *J. Geophys. Res.*, *106*, 65–76.
Taranenko, Y. N., U. S. Inan, and T. F. Bell (1993a), Interaction with the lower ionosphere of electromagnetic pulses from lightning: Heating, attachment, and ionization, *Geophys. Res. Lett.*, *20*, 1539–1542.
Taranenko, Y. N., U. S. Inan, and T. F. Bell (1993b), Interaction with the lower ionosphere of electromagnetic pulses from lightning: Excitation of optical emissions, *Geophys. Res. Lett.*, *20*, 2675–2678.
Vallance Jones, A. (1974), *Aurora*, pp. 87–134, Springer, New York.
Vaughan, O. H., Jr., R. J. Blakeslee, W. L. Boeck, B. Vonnegut, M. Brook, and J. McKune Jr. (1992), A cloud to space lighting as recorded by the space shuttle payload bay TV cameras, *Mon. Weather Rev.*, *120*, 1459.
Yair, Y., P. Israelevich, A. D. Devir, M. Moalem, C. Price, J. H. Joseph, Z. Levin, B. Ziv, A. Sternlieb, and A. Teller (2004), New observations of sprites from the space shuttle, *J. Geophys. Res.*, *109*, D15201, doi:10.1029/2003JD004497.
Yoshino, K., A. S.-C. Cheung, J. R. Esmond, W. H. Parkinson, D. E. Freeman, S. L. Guberman, A. Jenouvrier, B. Coquart, and M. F. Merienne (1988), Improved absorption cross-sections of oxygen in the wavelength region 205–240 nm of the Herzberg continuum, *Planet. Space Sci.*, *36*, 1469–1475.

A. B. Chen, R. R. Hsu, L. C. Lee, and H. T. Su, Department of Physics, National Cheng Kung University, Tainan 70148, Taiwan.
H. U. Frey and S. B. Mende, Space Science Laboratory, University of California, Berkeley, Berkeley, CA 94720, USA. (mende@ssl.berkeley.edu)
H. Fukunishi and Y. Takahashi, Department of Geophysics, Tohoku University, Aramaki-Aoba, Sendai 980-8578, Japan.
D. D. Sentman, Geophysical Institute, University of Alaska Fairbanks, Fairbanks, AK 99775, USA.